Journal of Materials Science Research; Vol. 3, No. 3; 2014
ISSN 1927-0585 E-ISSN 1927-0593
Published by Canadian Center of Science and Education

CdO Nanoparticles by Thermal Decomposition of a Cadmium-Hexamethylenetetramine Complex

Divine Mbom Yufanyi[1], Josepha Foba Tendo[1], Agwara Moise Ondoh[2] & Joseph Ketcha Mbadcam[2]

[1] Department of Chemistry, Faculty of Science, University of Buea, Buea, Cameroon

[2] Department of Inorganic Chemistry, Faculty of Science, University of Yaounde I, Yaounde, Cameroon

Correspondence: Josepha Foba Tendo, Department of Chemistry, Faculty of Science, University of Buea, P.O. Box 63, Buea, Cameroon. Tel: 237-7322-7719. E-mail: jnfoba@yahoo.com

Received: March 10, 2014 Accepted: March 24, 2014 Online Published: April 17, 2014

doi:10.5539/jmsr.v3n3p1 URL: http://dx.doi.org/10.5539/jmsr.v3n3p1

Abstract

CdO nanoparticles have been prepared by the thermal decomposition of a precursor complex. A simple and cost effective room temperature synthetic technique allows the preparation of the precursor complex from hexamethylenetetramine and cadmium nitrate in ethanol. The precursor, characterized by elemental analysis, mass spectrometry, Fourier transform infrared spectroscopy (FTIR), and thermal gravimetric analysis, had the composition [{Cd(HMTA)$(NO_3)_2(H_2O)_2$}n]. It was calcined at 500 ºC for 2 h, and the cadmium oxide nanoparticles obtained was characterized by X-ray diffraction (XRD), scanning electron microscopy, high resolution transmission electron microscopy (HRTEM), Nitrogen adsorption and physisorption, and Selected Area Electron Diffraction (SAED). XRD shows that the CdO obtained is pure and crystalline. The particles obtained had a cubic morphology and are mesoporous.

Keywords: cadmium oxide, hexamethylenetetramine, nanoparticles, thermal decomposition

1. Introduction

Over the past few decades, nanomaterials, including metal oxide nanoparticles, have received enormous scientific attention because of their interesting novel and improved physico-chemical and biological properties as a result of size reduction to the nano-regime (Devan, Patil, Lin, & Ma, 2012). Their unique physical properties that are size- and shape-dependent, render them applicable in many fields such as optics, magnetism, catalysis, electricity, energy production and storage, environmental remediation, antimicrobial agents and drug delivery (Mao, Park, Zhang, Zhou, & Wong, 2007; S. Wang, Z. Wang, & Zha, 2009; Jolivet et al., 2010). Among the different metal oxide nanoparticles, CdO is an important n-type semiconductor with a cubic structure, which belongs to the II–VI group, with a direct band gap of 2.5 eV and an indirect band gap of 1.98 eV (Tadjarodi & Imani, 2011b). The difference in band gap is attributed to intrinsic cadmium and oxygen vacancies. Due to its ionic nature coupled with its wide band gap, low electrical resistivity and high transmission in the visible region, CdO nanoparticles have been found to be a suitable candidate for application in various fields such as optical, photovoltaic cells, gas sensors, solar cells and front panel displays (Ye, Zhong, Zheng, R. Li, & Y. Li, 2007; Ghoshal et al., 2009; Tadjarodi & Imani, 2011b; Giribabu, Suresh, Manigandan, Stephen, & Narayanan, 2013; Kalpanadevi, Sinduja, & Manimekalai, 2013).

Given that the physico-chemical properties of CdO do not only depend on its chemical composition but also on size, shape and surface structure, the preparation of CdO nanoparticles of well-defined morphology and size is of interest. Synthesis techniques and conditions can considerably affect the properties of CdO nanoparticles. Several synthetic methods (physical, chemical and mechanical), including; hydrothermal method (Ye et al., 2007; Yang et al., 2010; Zhang, Wang, Lin, & Huang, 2010), template assisted method (Prakash, Arunkumar, Sathya Raj, & Jayaprakash, 2013), solvothermal methods (Ghoshal, Biswas, Nambissan, Majumdar, & De, 2009; Saghatforoush, Sanati, Mehdizadeh, & Hasanzadeh, 2012; Kaviyarasu, Manikandan, Paulraj, Mohamed, & Kennedy, 2014), mechano-chemical method (Tadjarodi & Imani, 2011a, 2011b), thermal decomposition (Shi, C. Wang, H. Wang, & Zhang, 2006; Gujar et al., 2008; Askarinejad & Morsali, 2009; Kumar et al., 2012), photosynthetic method (Andeani & Mohsenzadeh, 2013) and sonochemical method (Ramazani & Morsali, 2011; Safarifard & Morsali, 2012) have been employed to prepare CdO nanostructures. These different synthetic procedures have resulted in CdO nanoparticles of varying morphology such as nanowires (Ghoshal et al., 2009;

Yang et al., 2010), nanoplatelets (Giribabu et al., 2013), nanodisks (Shi et al., 2006), nanofibers (Ye et al., 2007), and nanorods (Barakat, Al-Deyab, & Kim, 2012; Kaviyarasu et al., 2014). Most of the synthetic techniques require expensive equipment, extra purification steps and long reaction times. For practical applications, the synthesis should be based on readily available, non-toxic and cheap precursors, as well as simple synthetic procedures without the necessity for additional purification steps.

The synthesis of CdO nanoparticles by thermal decomposition of organo-cadmium compounds or cadmium complexes has also been reported (Ramazani & Morsali, 2011; Ranjbar & Morsali, 2011; Safarifard & Morsali, 2012; Kalpanadevi, Sinduja, & Manimekalai, 2013; Payehghadr & Moasali, 2013). By proper choice of the precursor and the calcination conditions, this could be a simple and cost-effective technique for the preparation of oxide particles with controlled morphologies. However, the robustness and the reproducibility of the method is still a matter of concern.

Hexamethylenetetramine (HMTA) is a cheap and readily available heterocyclic organic compound with a cage-like structure. It is highly soluble in water and polar organic solvents. HMTA is a versatile ligand that can serve as a terminal monodentate or as bi-, tri-, and tetradentate bridging ligand (Kirillov, 2011). Apart from coordinative bonds, HMTA can also (depending on the synthesis conditions and the solvent used) be involved in the formation of hydrogen bonds (Ndifon et al., 2009). The kinetics of the thermal decomposition of some HMTA-transition metal complexes, leading to the formation of metal oxides (Mn, Ni, Zn, Cd) or metal nanoparticles in a carbon matrix (Ni, Co; Ni-Mo and Co-Mo carbides), have already been reported (Chouzier, Afanasiev, Vrinat, Cseri, & Roy-Auberger, 2006; Singh et al., 2007; Afanasiev et al., 2008; Chouzier et al., 2011; Kumar et al., 2012).

In this paper we report the synthesis and characterization (morphology and surface area) of CdO nanoparticles obtained by thermal decomposition of a Cd-HMTA precursor. The precursor was synthesized from simple, cheap, and relatively safer reagents. The synthetic process for both the precursor and the oxide nanoparticles is ecofriendly.

2. Method

2.1 Chemicals

$Cd(NO_3)_2 \cdot 6H_2O$, hexamethylenetetramine and ethanol were obtained from Sigma Aldrich. The chemicals were of analytical grade and were used without further purification.

2.2 Synthesis of the Cd-HMTA Precursor

The precursor was synthesized by modifying a procedure previously reported for a cadmium-HMTA polymeric complex (Kumar et al., 2012).

HMTA (4 mmol, 0.5608 g) was dissolved in 15 mL of ethanol (sonication for 20 min at room temperature). Cadmium nitrate (2 mmol) in 10 mL of ethanol was added drop wise under magnetic stirring. The mixture was stirred for a further 2 h. The white precipitate formed was filtered, washed several times with ethanol and dried in a desiccator over silica gel.

2.3 Synthesis of CdO Nanoparticle

A sample of the dry precursor (0.5 g) was ground, placed in a ceramic crucible and calcined at 500 °C (CdO-500). The crucible was placed in the furnace, heated to the desired calcination temperature, and calcination in air continued for 2 h. The sample was allowed to cool down to room temperature in the furnace. The reddish-brown powder obtained could easily be re-dispersed in water and ethanol.

2.4 Characterization Techniques

Elemental analysis (C, H, N) of the precursor was carried out on a Flash 2000 Thermo Scientific analyzer. Mass spectrometry of the precursor complex was performed on a Micro-Mass LCT Premier mass spectrometer (Waters Corporation, USA). FT-IR spectra were recorded from 4000 to 400 cm^{-1} on a PerkinElmer Spectrum Two universal attenuated total reflectance Fourier transform infrared (UATR-FT-IR) spectrometer. Thermogravimetric analysis (TGA) was obtained using a Pyris 6 PerkinElmer TGA 4000 thermal analyzer. The TGA analysis was conducted between 30 and 900 °C under nitrogen atmosphere at a flow rate of 20 mL/min and a temperature ramp of 10 °C/min. The XRD diffractogram of CdO was recorded on a Bruker D8 Advance X-ray diffractometer using a Cu Kα radiation source (λ = 0.15406 nm, 40 kV and 40 mA). Scans were taken over the 2θ range from 10^o to 100^o in steps of 0.01^o at room temperature in open quartz sample holders. The phase was identified with the help of the BrukerDIFFRACplus evaluation software in combination with the ICDD powder diffraction data base (International Centre for Diffraction Data). SEM images and EDX spectra were obtained on a JEOL

JSM-7600F field-emission scanning electron microscope. Transmission electron microscopy (TEM) was performed on a JEOL JEM-2100F microscope using a maximum acceleration voltage of 200 kV from the field emission gun. The particle size distribution was determined from the TEM image using the ImageJ software. N_2-physisorption experiment for the determination of the total surface area and the average pore diameter was conducted on a Micromeritics ASAP 2020 instrument. Prior to the measurement, the sample was degassed at 200 ˚C for 6 h.

3. Results and Discussion

The white and crystalline Cd-HMTA precursor was obtained from $Cd(NO_3)_2{\cdot}6H_2O$ and HMTA in ethanol at ambient conditions in one step. Light-brown CdO nanoparticles were obtained by calcination of the precursor at 500 ºC.

The elemental composition of the precursor (Table 1) corresponds closely to the empirical formula $CdC_6H_{16}N_6O_8$, which matches the structural formula $Cd(HMTA)(NO_3)_2(H_2O)_2$.

Table 1. Elemental analysis of the Cd-HMTA precursor compared to the values calculated for the empirical formula $CdC_6H_{16}N_6O_8$

Complex	Colour	% Yield	Elemental Analyses: % Found (% Calculated)			
			% Cd	% C	% H	% N
$Cd(HMTA)(NO_3)_2(H_2O)_2$	white	94	(27.24)	18.04 (17.46)	4.07 (3.91)	20.02 (20.37)

The high resolution mass spectrum (MS) of the complex shows a molecular ion (M^+-H) peak at m/z = 411.9 which corresponds to the structural formula derived from elemental analysis. Small peaks above m/z = 411.9 (473, 485, and 489) which correspond to the addition of water or nitrate fragments to the precursor, were also observed on the spectrum.

Table 2. Relevant FTIR bands of HMTA and the Cd-HMTA precursor

HMTA	$[\{Cd(HMTA)(NO_3)_2(H_2O)_2\}_n]$	Band Assignments
-	3480	ν(OH) (coordinated water)
2955	2950	ν(CH_2) stretch
-	1785	Cd-NO_3
1457	1432	ν(CH_2) scissor (HMTA)
1370	1380	ν(CH_2) wag (HMTA)
	1298	ν(CH_2) twist (HMTA)
	1241	ν(CH_2) rock (HMTA)
1235	1228	ν(CH_2) twist (HMTA)
1000	998	ν(CN) stretch (HMTA)
811	819	ν(CN) stretch (HMTA)
670	682	N-C-N bend (HMTA)
-	505	Cd-O stretch

Relevant infrared bands of HMTA and the precursor complex are listed in Table 2. The broad band at 3480 cm^{-1} in the FTIR spectrum of Cd-HMTA (Figure 1) is attributed to ν(OH) of coordinated water (Hee Ng, Guan Teoh, Moris, & Yang Yap, 2004; Ndifon et al., 2009). The band at 1235 cm^{-1}, assigned to the C-N stretching vibration of the free HMTA ligand is split into 1241 and 1228 cm^{-1} in the Cd-HMTA precursor suggesting that HMTA is coordinated to the cadmium ion (Ndifon et al., 2009). Strong prominent peaks at 811 and 1000 cm^{-1} due to the C-N stretching vibration of HMTA (Jensen, 2002) are shifted to 819 and 998 cm^{-1}, respectively in the Cd-HMTA

precursor complex. The weak band observed at 1785 cm^{-1} shows the coordination of a monodentate nitrate ion, Cd-NO_3 (Ndifon et al., 2009). The coordination of water molecules is also indicated by the IR bands in the region 400–600 cm^{-1}, assigned to Cd-H_2O (Ndifon et al., 2009). The elemental, mass spectrum and FTIR analytical results indicate that the complex is probably polymeric with formula $[\{Cd(HMTA)(NO_3)_2(H_2O)_2\}_n]$.

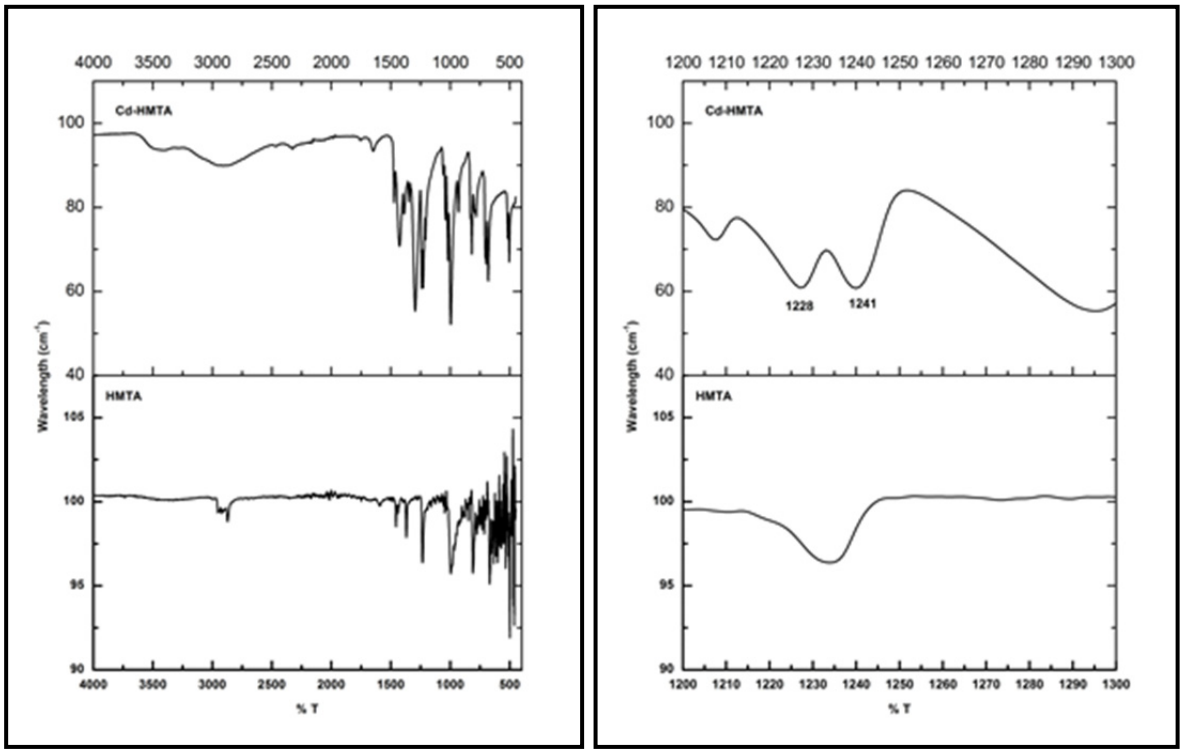

Figure 1. a) FTIR spectra of HMTA and Cd-HMTA precursor complex; b) Expansion of FTIR spectrum in region 1200–1300 cm^{-1} to show split of band

The thermal decomposition curve of the Cd-HMTA precursor is shown in Figure 2 while the relevant decomposition data are summarized in Table 3.

Table 3. Thermal decomposition data for Cd-HMTA precursor

Step	Temperature Range (ºC)	% Mass Loss
1	150–190	6.8
2	200–400	41.4
3	400–630	18.7

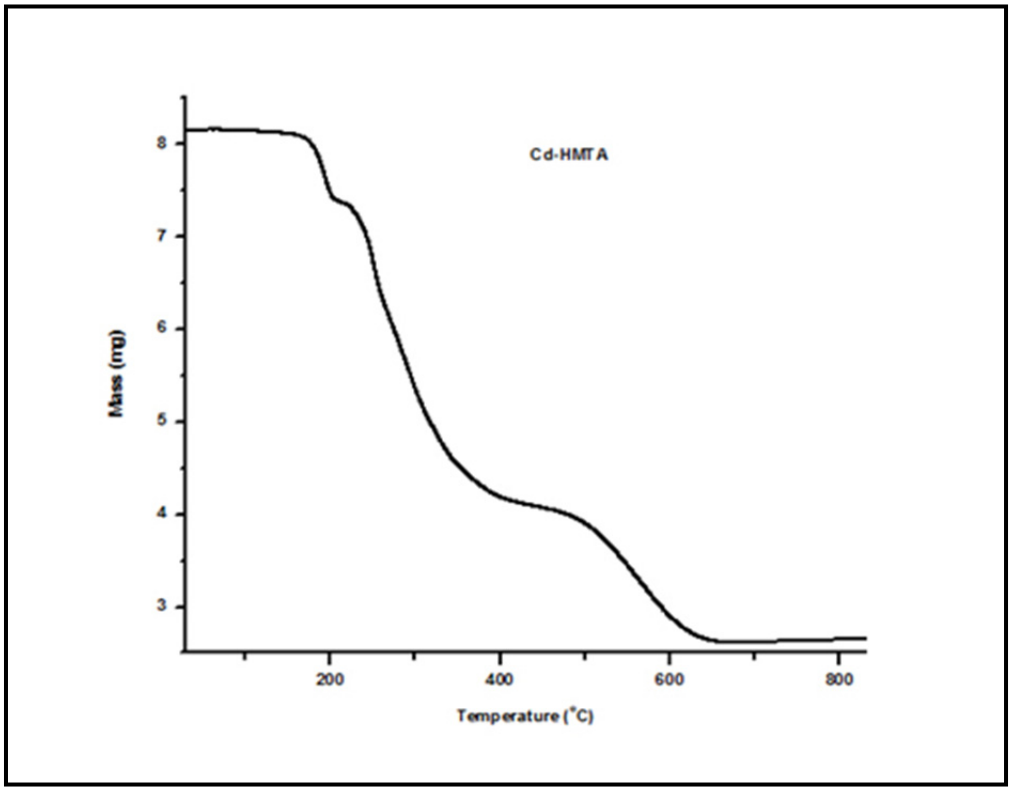

Figure 2. Thermogravimetric analysis of Cd-HMTA precursor complex

The precursor $Cd(HMTA)(NO_3)_2(H_2O)_2$ is composed of 27.25% Cd, 8.72% H_2O, 33.95% HMTA and 30.07% NO_3^-. The TG curve (Figure 2) shows that the precursor decomposes in three major steps within the temperature range 30–830 °C. However, the derivative TG indicates that the pattern is complex; in the range 200–400 °C there are two overlapping decomposition steps and not one (indicated by a strong narrow peak and a weak shallow peak).

The first decomposition step between 150–190 °C which is distinctive (mass loss of 6.8%), can be attributed predominantly to the loss of water (calc. 8.7%). This discrepancy suggests that water may not be lost as molecular water. The major mass loss of 41.4% takes place in the range 200–400 °C. This could be assigned to the decomposition of HMTA and part of the nitrate in the form of various gases (Afanasiev et al., 2008). This assignment is supported by the observation that in this range, the derivative TG indicates that there are two overlapping decomposition steps and not one. The coordination of HMTA to Cd tends to weaken the Cd-NO_3^- bond, suggesting that the bonding environment of the nitrates is not identical and thus will decompose at different temperatures. We propose that the extensively H-bonded nitrates decompose at slightly lower temperatures than the covalently bonded ones. Over the range 400–630 ºC we have another distinctive decomposition step with a mass loss of 18.7% which can be assigned to the decomposition of the remaining nitrate. A stable mass is obtained at 630 °C with 32.1% residue (calc. 31.3%), which is predominantly CdO due to the oxidative nature of the environment (presence of water vapour).

The calcination temperature was chosen as 500 °C from the derivative TG plot which indicates that 550 °C is the optimum temperature. This temperature is lower than that indicated by the TG (630 °C). This is probably due to the use of a fast heating rate (10 °C per minute) which permits a base-line drift further away from equilibrium conditions because a short time is required for each determination.

The XRD pattern of CdO obtained is shown in Figure 3. The sharp and well defined peaks indicate the crystalline nature of CdO. The strong diffraction peaks in the XRD spectrum of CdO occurring at 2θ values of 33.00, 38.29, 55.27, 65.87, 69.24, and 81.95 are indexed as the (111), (200), (220), (311), (222), and (400) crystal planes and correspond to the cubic structure of CdO (JCPDS card No. 65-2908). No other impurity peaks were detected indicating that the obtained CdO was phase pure. The average particle size of CdO was calculated using Debye-Scherrer equation (Equation 1) (Klug & Alexander, 1974):

$$D = k\lambda/\beta \mathrm{Sin}\theta \quad (1)$$

Where D is the average particle size, λ is the X-ray wavelength, β is the corrected width of the XRD peak at half height, k is the shape factor which is approximated as 0.89, and θ is the Bragg diffraction angle. The calculated average particle size of cadmium oxide nanoparticles was found to be 30.9 nm.

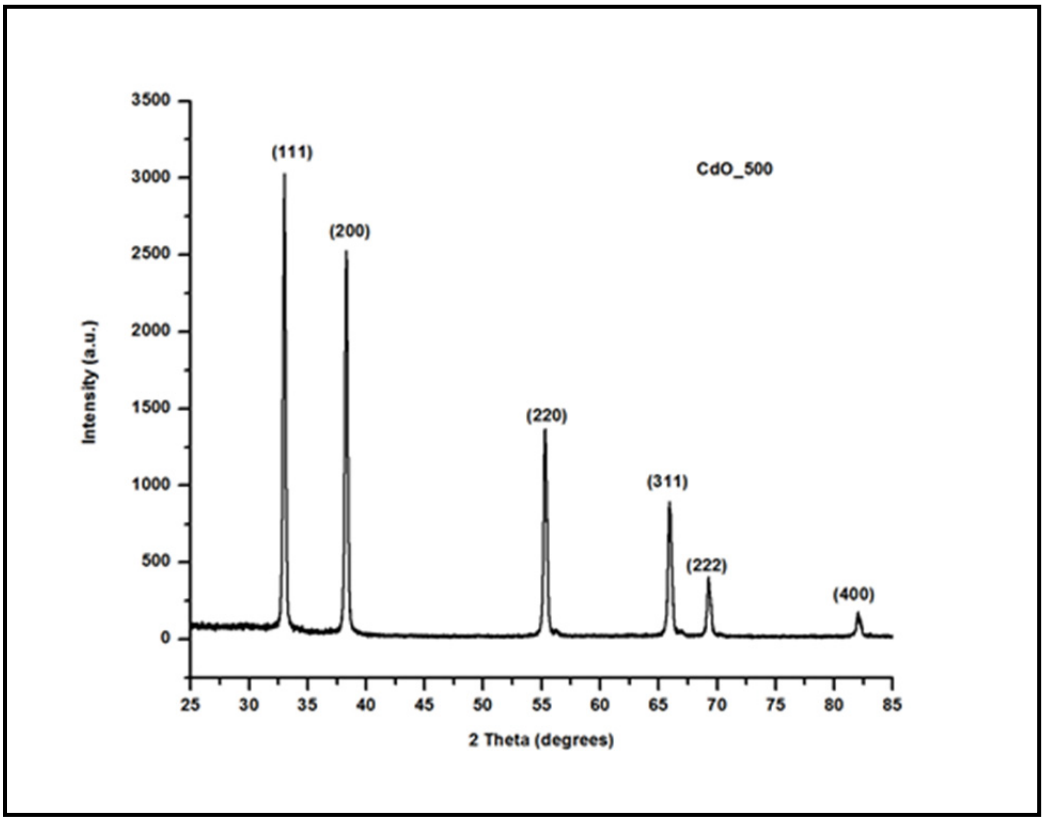

Figure 3. XRD pattern of CdO nanoparticles

The morphology and structural features of CdO nanoparticles were determined by SEM, TEM and SAED. The SEM image (Figure 4a) indicates that the Cd-HMTA precursor has a spike-shaped morphology, while the CdO nanoparticles have rod-like morphology. The EDX spectrum of the precursor (Figure 4c) indicates that it contains only Cd, C, H, N, and O, while that of CdO (Figure 4d) indicates pure CdO is obtained. The Cu impurity found in the EDX of CdO is due to the sample holder.

The HRTEM image (Figure 5a) of CdO shows particles with a cubic shape. The larger particles present are due to aggregation or the overlapping of small particles. The average particle diameter of 22.7 nm for CdO was determined after a log normal fitting of the data obtained from the TEM image. The resulting histogram and average particle size are shown in Figure 6a. The average particle size from HRTEM is consistent with values obtained by XRD. The SAED image of CdO (Figure 5b) shows bright spots which indicate that the CdO nanoparticles are polycrystalline in nature.

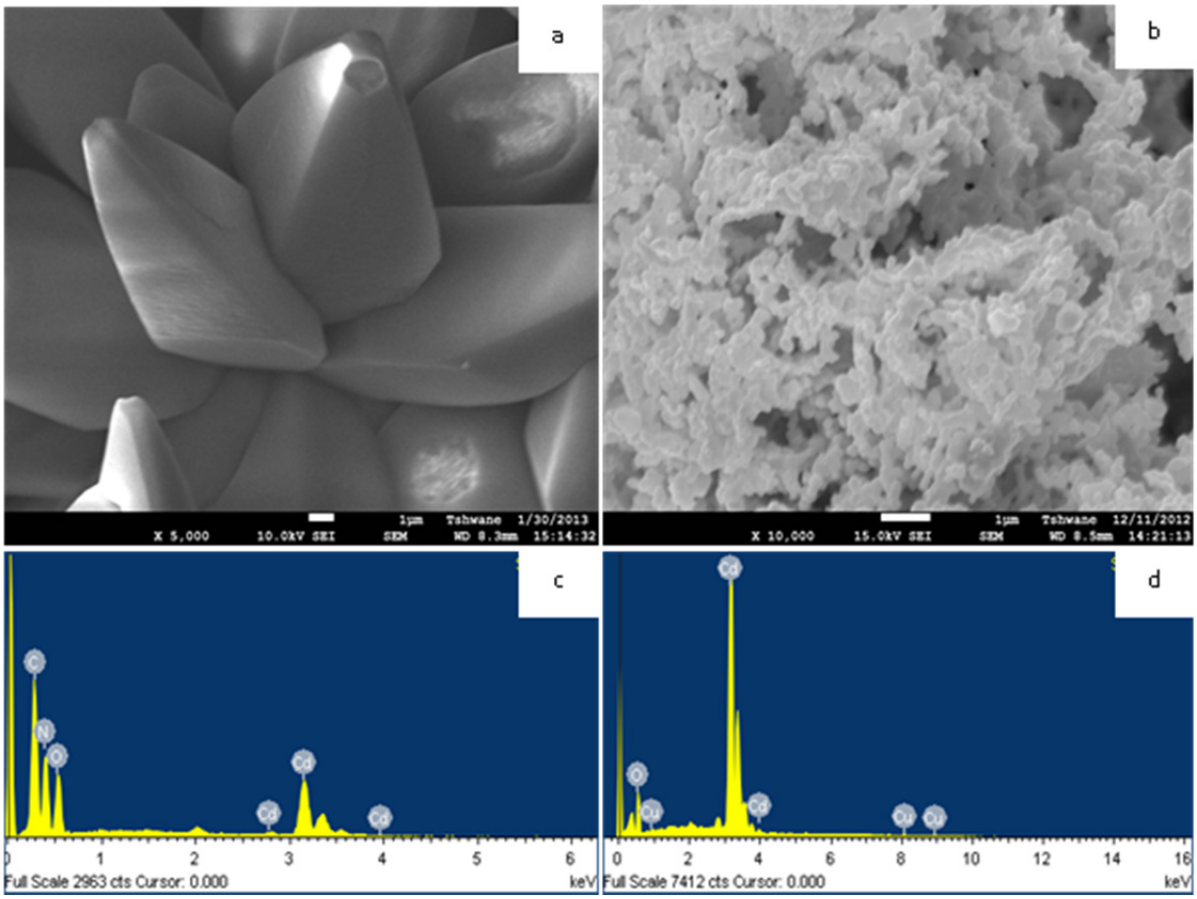

Figure 4. SEM images of (a) Cd-HMTA precursor and (b) CdO; EDX images of (c) Cd-HMTA precursor and (d) CdO

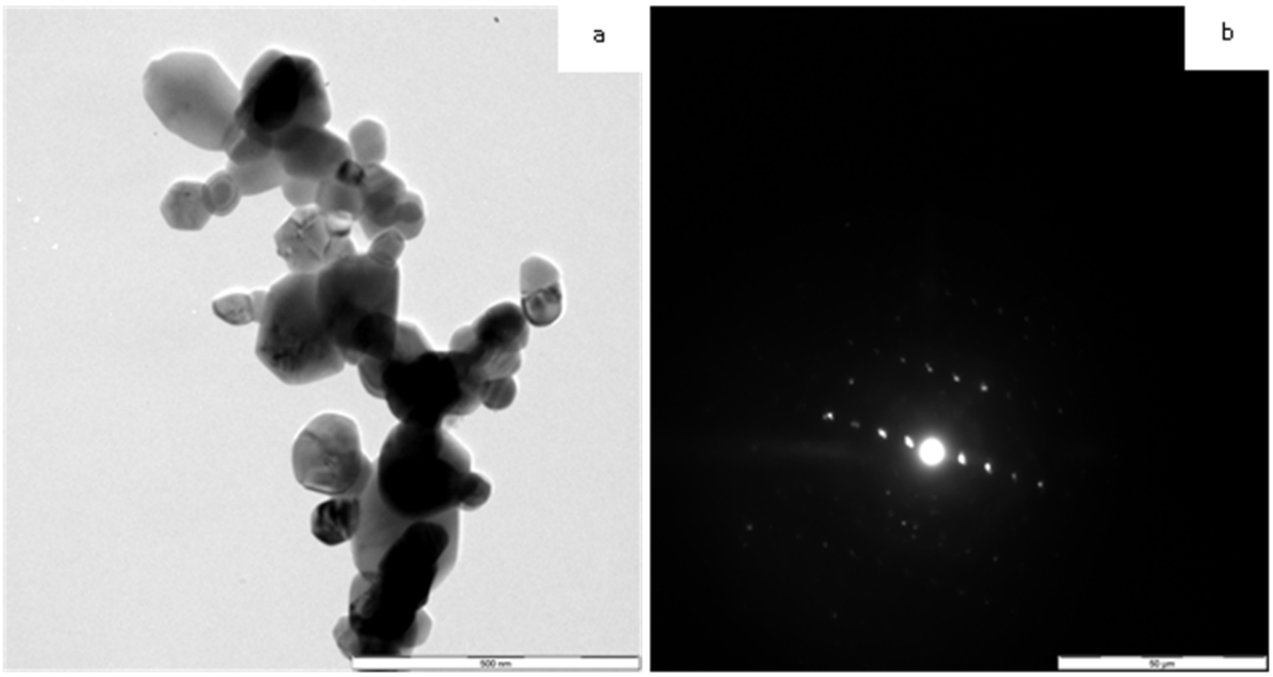

Figure 5. (a) TEM image and (b) SAED image of CdO nanoparticle

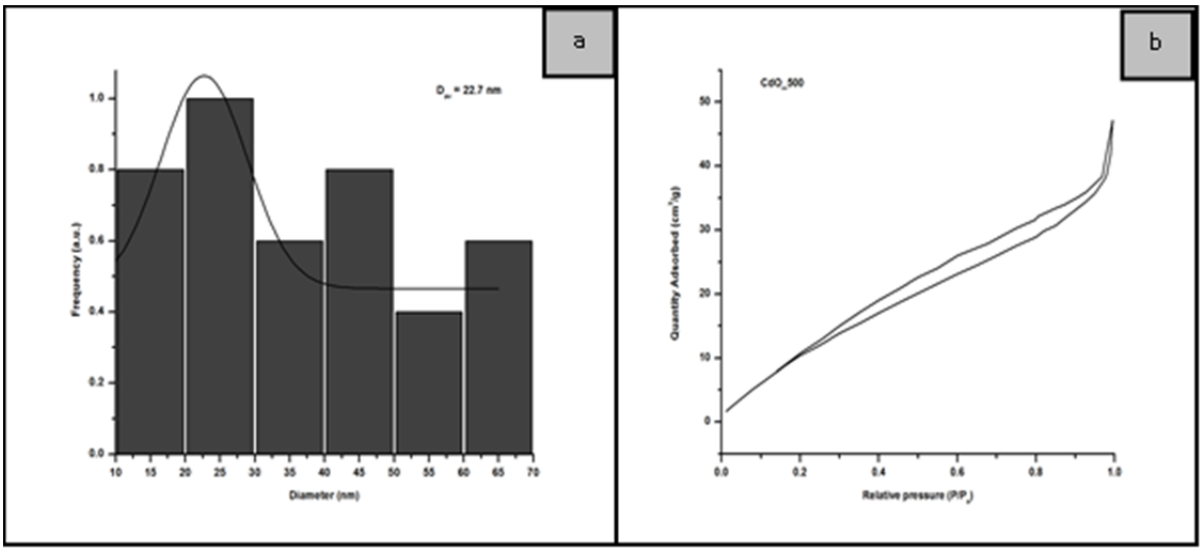

Figure 6. (a) Particle size distribution and (b) N_2 adsorption/desorption isotherm for CdO nanoparticles

For comparison, some CdO particle morphologies and sizes found in the literature that are obtained by the thermal decomposition of different precursors are listed in Table 4. The results indicate that cubic nanoparticles with sizes in the range 10–70 nm obtained from the Cd-HMTA precursor of this study compares favorably with those obtained from other starting materials. It can also be observed from Table 4 that our starting materials are the simplest, most readily available, and very cost-effective.

Table 4. Particle sizes (HRTEM) of CdO prepared by the thermal decomposition of various precursors at different calcination temperatures

Precursor	Calcination		Particle Size (HRTEM) (nm)	Morphology	Ref.
	Time (h)	Temperature (ºC)			
$Cd(CH_3COO)_2{\cdot}2H_2O$ + $CO(NH_2)_2$	2	500	46	Spherical	(Tadjarodi et al., 2013)
$Cd(Cin)_2{\cdot}(N_2H_4)_2$	0.45	500	31	Cubic	(Kalpanadevi et al., 2013)
$Cd(CH_3COO)_2{\cdot}2H_2O$ + PEG-400 + NaOH	1	400	15–36	/	(Liu et al., 2011)
$[Cd(L)_2(H_2O)_2]$	4	650	/	Agglomerated particles	(Safarifard & Morsali, 2012)
Cis-[dmphen-CdI_2]	2	400	50	Spherical	(Aldwayyan et al., 2013)
$[\{Cd(HMTA)(NO_3)_2(H_2O)_2\}_n]$	2	500	10–70	Cubic	This work

Cin = Cinnamic acid; PEG = polyethylene glycol; L = 1H-1,2,4-triazole-3-carboxylate; dmphen = 2,9-dimethyl-1,10-phenanthroline

The surface area and average pore size distribution (PSD) of CdO nanoparticles were determined by N_2 physisorption. The nitrogen adsorption–desorption isotherms (Figure 6b) of CdO can be classified as type IV with H3 hysteresis loop (according to the IUPAC classification) (Greg & Sing, 1982). The isotherm type and hysteresis loop observed here indicates that CdO nanoparticles possess slit mesoporous structure (Greg & Sing, 1982). The BET surface area (according to Brunauer, Emmett and Teller) of CdO was found to be 58.4 m^2/g and the pore volume 0.059 cm^3/g. The Barrett-Joyner-Halenda (BJH) desorption pore size distribution of 4.7 nm indicates a mesoporous structure for the CdO nanoparticles with high surface contact sites.

4. Conclusion

Pure, crystalline and cubic CdO nanoparticles have been synthesized by the thermal decomposition of a Cd-HTMA precursor. The TG curve indicates the precursor decomposes in three steps but the derivative TG suggests the second decomposition step is composed of two overlapping steps instead of one. This renders the decomposition pattern more complex. The metal oxide nanoparticles were confirmed by XRD and calculated to have average size 30.9 nm. The morphology of the oxide nanoparticles (cubic) is different from that of the precursor (spikelike) and they have sizes in the range 10–70 nm. The average size of 22.7 nm for the nanoparticles is lower or compares favorably with those obtained by the decomposition of more expensive or less readily available starting materials. The CdO nanoparticles obtained is mesoporous, has a surface area of 58.4 m^2/g and an average pore diameter of 4.7 nm. The low-temperature synthetic technique is simple and cost effective and it can be extended to the synthesis of other metal oxide nanoparticles.

Acknowledgments

The authors thank Dr. Khamlich Saleh (University of Pretoria) for assistance with the SEM and TEM images.

References

Afanasiev, P., Chouzier, S., Czeri, T., Pilet, G., Pichon, C., Roy, M., & Vrinat, M. (2008). Nickel and Cobalt Hexamethylentetramine Complexes $(NO_3)_2Me(H_2O)_6(HMTA)_2{\cdot}4H_2O$ (Me = Co^{2+}, Ni^{2+}): New Molecular Precursors for the Preparation of Metal Dispersions. *Inorganic Chemistry, 47*(7), 2303-2311. http://dx.doi.org/10.1021/ic7013013

Aldwayyan, A. S., Al-Jekhedab, F. M., Al-Noaimi, M., Hammouti, B., Hadda, T. B., Suleiman, M., & Warad, I. (2013). Synthesis and Characterization of CdO Nanoparticles Starting from Organometalic Dmphen-CdI_2 complex. *International Journal of Electrochemical Science, 8*, 10506-10514. Retrieved from http://www.electrochemsci.org/papers/vol8/80810506.pdf

Andeani, J. K., & Mohsenzadeh, S. (2013). Phytosynthesis of Cadmium Oxide Nanoparticles from Achillea wilhelmsii Flowers. *Journal of Chemistry, 2013*, 1-4. http://dx.doi.org/10.1155/2013/147613

Askarinejad, A., & Morsali, A. (2009). Synthesis of cadmium(II) hydroxide, cadmium(II) carbonate and cadmium(II) oxide nanoparticles; investigation of intermediate products. *Chemical Engineering Journal, 150*(2), 569-571. http://dx.doi.org/10.1016/j.cej.2009.03.005

Barakat, N. A. M., Al-Deyab, S., & Kim, H. Y. (2012). Synthesis and study of the photoluminescence and optical characteristics of Cd/CdO nanorods prepared by the electrospinning process. *Materials Letters, 66*(1), 225-228. http://dx.doi.org/10.1016/j.matlet.2011.08.074

Chouzier, S., Afanasiev, P., Vrinat, M., Cseri, T., & Roy-Auberger, M. (2006). One-step synthesis of dispersed bimetallic carbides and nitrides from transition metals hexamethylenetetramine complexes. *Journal of Solid State Chemistry, 179*(11), 3314-3323. http://dx.doi.org/10.1016/j.jssc.2006.06.026

Chouzier, S., Czeri, T., Roy-Auberger, M., Pichon, C., Geantet, C., Vrinat, M., & Afanasiev, P. (2011). Decomposition of molybdate–hexamethylenetetramine complex: One single source route for different catalytic materials. *Journal of Solid State Chemistry, 184*(10), 2668-2677. http://dx.doi.org/10.1016/j.jssc.2011.08.005

Devan, R. S., Patil, R. A., Lin, J. -H., & Ma, Y. -R. (2012). One-Dimensional Metal-Oxide Nanostructures: Recent Developments in Synthesis, Characterization, and Applications. *Advanced Functional Materials, 22*(16), 3326-3370. http://dx.doi.org/10.1002/adfm.201201008

Ghoshal, T., Biswas, S., Nambissan, P. M. G., Majumdar, G., & De, S. K. (2009). Cadmium Oxide Octahedrons and Nanowires on the Micro-Octahedrons: A Simple Solvothermal Synthesis. *Crystal Growth & Design, 9*(3), 1287-1292. http://dx.doi.org/10.1021/cg800203y

Giribabu, K., Suresh, R., Manigandan, R., Stephen, A., & Narayanan, V. (2013). Cadmium oxide nanoplatelets: synthesis, characterization and their electrochemical sensing property of catechol. *Journal of Iranian Chemical Society, 10*, 771-776. http://dx.doi.org/10.1007/s13738-012-0211-3

Greg, S. J., & Sing, K. S. W. (1982). *Adsorption, Surface Area and Porosity* (2nd ed.). Academic Press.

Gujar, T. P., Shinde, V. R., Kim, W. -Y., Jung, K. -D., Lokhande, C. D., & Joo, O. -S. (2008). Formation of CdO films from chemically deposited $Cd(OH)_2$ films as a precursor. *Applied Surface Science, 254*(13), 3813-3818. http://dx.doi.org/10.1016/j.apsusc.2007.12.015

Hee Ng, C., Guan Teoh, S., Moris, N., & Yang Yap, S. (2004). Structural, infrared spectral and

thermogravimetric analysis of a hydrogen-bonded assembly of cobalt(II) and nickel(II) mixed complex cations with hexamethylenetetraamine and aqua ligands: $\{[M(hmt)_2(H_2O)_4][M(H_2O)_6]\}(SO_4)_2{\cdot}6H_2O$. *Journal of Coordination Chemistry, 57*(12), 1037-1046. http://dx.doi.org/10.1080/00958970412331281791

Jensen, J. O. (2002). Vibrational frequencies and structural determinations of hexamethylenetetraamine. *Spectrochimica Acta Part A: Molecular and Biomolecular Spectroscopy, 58*(7), 1347-1364. http://dx.doi.org/10.1016/S1386-1425(01)00585-6

Jolivet, J. -P., Cassaignon, S., Chaneac, C., Chiche, D., Durupthy, O., & Portehault, D. (2010). Design of metal oxide nanoparticles: Control of size, shape, crystalline structure and functionalisation by aqueous chemistry. *C.R. Chimie, 13*, 40-51. http://dx.doi.org/10.1016/j.crci.2009.09.012

Kalpanadevi, K., Sinduja, C. R., & Manimekalai, R. (2013). Characterisation of Zinc Oxide and Cadmium Oxide Nanostructures Obtained from the Low Temperature Thermal Decomposition of Inorganic Precursors. *ISRN Inorganic Chemistry, 2013*, 1-5. http://dx.doi.org/10.1155/2013/823040

Kaviyarasu, K., Manikandan, E., Paulraj, P., Mohamed, S. B., & Kennedy, J. (2014). One dimensional well-aligned CdO nanocrystal by solvothermal method. *Journal of Alloys and Compounds, 593*, 67-70. http://dx.doi.org/10.1016/j.jallcom.2014.01.071

Kirillov, A. M. (2011). Hexamethylenetetramine: An old new building block for design of coordination polymers. *Coordination Chemistry Reviews, 255*(15–16), 1603-1622. http://dx.doi.org/10.1016/j.ccr.2011.01.023

Klug, H. P., & Alexander, L. E. (1974). *X-ray Diffraction Procedures for Polycrystalline and Amorphous Materials*. New York: Wiley.

Kumar, D., Kapoor, I. P. S., Singh, G., Goel, N., & Singh, U. P. (2012). Preparation, characterization and thermal behaviour of polymeric complex of cadmium hexamethylenetetramine nitrate. *Solid State Sciences, 14*, 495-500. http://dx.doi.org/10.1016/j.solidstatesciences.2012.01.021

Liu, J., Zhao, C., Li, Z., Yu, L., Li, Y., Gu, S., … Yang, C. (2011). Solid State Synthesis and Optical properties-Controlling Studies of CdO Nanoparticles. *Advanced Materials Research, 228-229*, 580-585. http://dx.doi.org/10.4028/www.scientific.net/AMR.228-229.580

Mao, Y., Park, T. -J., Zhang, F., Zhou, H., & Wong, S. S. (2007). Environmentally Friendly Methodologies of Nanostructure Synthesis. *Small, 3*(7), 1122-1139. http://dx.doi.org/10.1002/smll.200700048

Ndifon, P. T., Agwara, M. O., Paboudam, A. G., Yufanyi, D. M., Ngoune, J., Galindo, A., … Mohamadou, A. (2009). Synthesis, characterisation and crystal structure of a cobalt(II)-hexamethylenetetramine coordination polymer. *Transition Metal Chemistry, 34*(7), 745-750. http://dx.doi.org/10.1007/s11243-009-9257-1

Payehghadr, M., & Moasali, A. (2013). Thermolysis preparation of cadmium(II) oxide nanoparticles from a new three-dimensional cadmium(II) supramolecular compound. *Journal of Structural Chemistry, 54*(4), 787-791. http://dx.doi.org/10.1134/s0022476613040197

Prakash, T., Arunkumar, T., Sathya Raj, D., & Jayaprakash, R. (2013). Surfactant-liaised Variation in CdO Nanocomposites Morphology. *Physics Procedia, 49*, 36-43. http://dx.doi.org/10.1016/j.phpro.2013.10.008

Ramazani, M., & Morsali, A. (2011). Sonochemical syntheses of a new nano-plate cadmium(II) coordination polymer as a precursor for the synthesis of cadmium(II) oxide nanoparticles. *Ultrasonics Sonochemistry, 18*(5), 1160-1164. http://dx.doi.org/10.1016/j.ultsonch.2010.12.011

Ranjbar, Z. R., & Morsali, A. (2011). Ultrasound assisted syntheses of a nano-structured two-dimensional mixed-ligand cadmium(II) coordination polymer and direct thermolyses for the preparation of cadmium(II) oxide nanoparticles. *Polyhedron, 30*(6), 929-934. http://dx.doi.org/10.1016/j.poly.2010.12.033

Safarifard, V., & Morsali, A. (2012). Sonochemical syntheses of a nanoparticles cadmium(II) supramolecule as a precursor for the synthesis of cadmium(II) oxide nanoparticles. *Ultrasonics Sonochemistry, 19*(6), 1227-1233. http://dx.doi.org/10.1016/j.ultsonch.2012.02.013

Saghatforoush, L. A., Sanati, S., Mehdizadeh, R., & Hasanzadeh, M. (2012). Solvothermal synthesis of $Cd(OH)_2$ and CdO nanocrystals and application as a new electrochemical sensor for simultaneous determination of norfloxacin and lomefloxacin. *Superlattices and Microstructures, 52*(4), 885-893. http://dx.doi.org/10.1016/j.spmi.2012.07.019

Shi, W., Wang, C., Wang, H., & Zhang, H. (2006). Hexagonal Nanodisks of Cadmium Hydroxide and Oxide

with Nanoporous Structure. *Crystal Growth & Design, 6*(4), 915-918. http://dx.doi.org/10.1021/cg050431z

Singh, G., Baranwal, B. P., Kapoor, I. P. S., Kumar, D., & Fröhlich, R. (2007). Preparation, X-ray Crystallography, and Thermal Decomposition of Some Transition Metal Perchlorate Complexes of Hexamethylenetetramine. *The Journal of Physical Chemistry A, 111*(50), 12972-12976. http://dx.doi.org/10.1021/jp077278z

Tadjarodi, A., & Imani, M. (2011a). A novel nanostructure of cadmium oxide synthesized by mechanochemical method. *Materials Research Bulletin, 46*(11), 1949-1954. http://dx.doi.org/10.1016/j.materresbull.2011.07.016

Tadjarodi, A., & Imani, M. (2011b). Synthesis and characterization of CdO nanocrystalline structure by mechanochemical method. *Materials Letters, 65*(6), 1025-1027. http://dx.doi.org/10.1016/j.matlet.2010.12.054

Tadjarodi, A., Imani, M., & Kerdari, H. (2013). Application of a facile solid-state process to synthesize the CdO spherical nanoparticles. *International Nano Letters, 3*(43), 1-6. http://dx.doi.org/10.1186/2228-5326-3-43

Wang, S., Wang, Z., & Zha, Z. (2009). Metal nanoparticles or metal oxide nanoparticles, an efficient and promising family of novel hetrogeneous catalysts in organic synthesis. *Dalton Transactions*, 9363-9373. http://dx.doi.org/10.1039/b913539a

Yang, Z. -X., Zhong, W., Yin, Y. -X., Du, X., Deng, Y., Au, C., & Du, Y. -W. (2010). Controllable Synthesis of Single-Crystalline CdO and $Cd(OH)_2$ Nanowires by a Simple Hydrothermal Approach. *Nanoscale Research Letters, 5*, 961-965. http://dx.doi.org/10.1007/s11671-010-9589-y

Ye, M., Zhong, H., Zheng, W., Li, R., & Li, Y. (2007). Ultralong Cadmium Hydroxide Nanowires: Synthesis, Characterization, and Transformation into CdO Nanostrands. *Langmuir, 23*(17), 9064-9068. http://dx.doi.org/10.1021/la070111c

Zhang, J., Wang, Y., Lin, Z., & Huang, F. (2010). Formation and Self-Assembly of Cadmium Hydroxide Nanoplates in Molten Composite-Hydroxide Solution. *Crystal Growth & Design, 10*(10), 4285-4291. http://dx.doi.org/10.1021/cg901559y